Finite-size effect on Néel temperature in antiferromagnetic nanoparticles

X. G. Zheng*
Department of Physics, Saga University, Saga 840-8502, Japan

C. N. Xu and K. Nishikubo
National Institute of Advanced Industrial Science and Technology, Tosu, Saga 841-0052, Japan

K. Nishiyama and W. Higemoto
Meson Science Laboratory, Institute of Material Structure Science, High Energy Accelerator Research Organization (KEK-MSL), Ibaraki 305-0801, Japan

W. J. Moon and E. Tanaka
High Voltage Electron Microscopy Laboratory, Kyushu University, Fukuoka 812-8512, Japan

E. S. Otabe
Department of Computer Science and Electronics, Faculty of Computer Science and Systems Engineering, Kyushu Institute of Technology, Fukuoka 820-8502, Japan

(Received 6 December 2004; revised manuscript received 7 February 2005; published 28 July 2005)

Muon spin relaxation/rotation (μSR) and magnetic susceptibility measurements were carried out on antiferromagnetic nanoparticles of CuO. Nanoparticles with center size of around 5 nm were prepared by ball-milling from single crystals of CuO and investigated using μSR measurements. In the ~5 nm assembly, the T_N was reduced drastically to ~30 K, compared with the bulk T_N=229 K. A similar effect was observed in a system of 2 to 3 nm diameter nanorods, which was synthesized by a direct solution reaction method, where T_N was suppressed further to 13 K. The present work reports direct evidence of a dramatic finite-size effect on the magnetic transition temperature in antiferromagnetic systems.

DOI: 10.1103/PhysRevB.72.014464 PACS number(s): 75.75.+a, 75.70.−i, 76.75.+i, 76.90.+d

I. INTRODUCTION

Finite-size effects in magnetic materials (ferromagnets and antiferromagnets) have received much attention in recent years. They reflect deviations from bulk properties as their sample dimensions are reduced. For systems with long correlation lengths, such as traditional superconductors having coherence lengths on the order of hundreds of angstroms, reduction of the superconducting transition temperature caused by finite-size effects has been observed in numerous systems.[1] In strongly correlated systems with short correlation lengths, such as ferromagnets and antiferromagnets, finite-size effects in the magnetic transition temperature, T_C (Curie temperature) or T_N (Néel temperature), are visible only in ultrathin films or nanoparticles. In a simple model of mean field theory, the magnetic transition temperature depends on the strength of the exchange interaction and the number of neighboring atoms. Therefore, reduction of the magnetic transition temperatures on the surface is expected. For example, in this model, the (110) surface for a face-centered-cubic ferromagnet with isotropic exchange interaction would be expected to have a surface T_C of 7/12 bulk T_C if the surface were not coupled to the bulk. However, this simple estimation is incorrect and the surface T_C in practical magnetic systems has been considered as nearly equivalent to the bulk value.[2]

Recently, drastic reduction of the Curie temperature (T_C) has been reported in ferromagnetic ultrathin films of a few monolayers, such as that of cobalt.[3] An experiment using the surface magneto-optical Kerr effect on ultrathin films of cobalt showed a drastic decrease in T_C from over 1000 K to below 50 K, and a strong influence of substrate topology on T_C.[3] However, this result contradicts those of the same experiment by another group, which found no change in the T_C for 1 monolayer Co up to 430 K.[4] In these ferromagnetic materials, high values of T_C (T_C>1000 K) prevent determination of T_C without first degrading the ultrathin film. On a low T_C ferromagnet of Tb nanoparticles [T_C (bulk)=222 K], drastic reduction in magnetic transition temperature was observed through dc magnetization measurements with a weak applied magnetic field after zero-field cooling (ZFC).[5] On another low T_C ferromagnet of Gd [T_C (bulk)=292.5 K], only a moderate reduction with T_C (1 monolayer)=0.9 T_C (bulk) was monitored by magnetic resonance,[6] even though an observation of T_C dropping below 120 K was made with the ac susceptibility measurement.[7] As detailed below regarding antiferromagnets, weak-field magnetic susceptibility measurement under zero-field-cooling condition often detects an extrinsic thermal blocking temperature T_B rather than the actual transition temperature.

Chemically stable antiferromagnetic systems such as CoO and NiO are more suitable to investigate this finite-size effect. Previous zero-field-cooled magnetic susceptibility studies of thin layers of CoO and resistivity measurements in Cr/Fe multilayers have shown drastic reductions in the magnetic transition temperature T_N (e.g., "T_N" was reduced from the bulk 291 K to "T_N" =25 K for 1.5 nm film CoO).[8,9] Similar effects for T_N were found for MnO and CoO

nanoparticles by electron spin resonance (ESR) measurements.[10,11] However, the latter method was an indirect method that used extrapolation from the paramagnetic range. "T_N" was produced by fitting the temperature dependence of the ESR linewidth ΔH to an assumption where ΔH was assumed to approach $T/(T-T_N)$ near T_N.[10,11] Nevertheless, recent thermodynamic measurements on CoO and NiO showed only a moderate 10% reduction of the T_N for ultrathin films.[12,13] A neutron diffraction study on NiO nanoparticle discs with an average diameter of 12 nm and a thickness of 2 nm indicated a moderate 12% reduction in T_N, in agreement with an extended mean field model.[14] A study on Fe_3O_4/CoO systems showed that the "transition temperature," as determined from the ZFC susceptibility measurements, approached zero in a linear manner with a decreasing thickness of CoO. In contrast, the intrinsic T_N, as determined from the neutron diffraction, actually increased with a decreasing CoO thickness (because of the proximity of magnetic Fe_3O_4 layers).[15] These results strongly imply that the magnetic susceptibility measurement under a zero-field cooling condition may only monitor an extrinsic blocking temperature T_B.[12,13,15]

Classically, ferromagnetic particles with dimensions of about 10–20 nm become superparamagnetic and are subject to spontaneous flips of magnetization by thermal activation. For antiferromagnetic materials, Néel suggested that antiferromagnetic nanoparticles might show superparamagnetism because of uncompensated spins on the surface; at a characteristic temperature T_B, the thermal flips are blocked so that coercivities and hysteresis loops are observed for antiferromagnetic nanoparticles.[16] As indicated in Ref. 13, when these uncompensated surface spins are tightly coupled to the spins inside the nanoparticles, they might serve as a measure of the transition temperature T_N. However, they might dominate the magnetic measurements without providing information about the intrinsic magnetic property of nanoparticles when they are coupled loosely. This domination of measurement explains the discrepancy between CoO results obtained by the ZFC magnetic susceptibility technique and by specific heat or neutron diffraction measurements. A similar magnetic blocking effect has been observed extensively in antiferromagnet/ferromagnet interfaces, where it is clarified in detail that blocking temperature T_B is generally lower than the real transition temperature and can be influenced by numerous other extrinsic parameters such as the grain/layer size and surface roughness.[17] Nanoparticle ferromagnetic particles are known to become superparamagnetic. At low temperatures, thermal blocking of the superparamagnetism might occur. Therefore, results by ZFC magnetic susceptibility measurement might be obscure. Therefore, whether a drastic finite-size effect on the magnetic transition temperature appears in magnetic systems remains an open issue and an enriched category of materials would be desirable.

Based on the above information, this study examines antiferromagnetic CuO systems using muon spin relaxation/rotation method (μSR). The μSR directly detects changes in the internal field. Consequently, it detects the intrinsic magnetic phase transition. Compared to the neutron diffraction technique, which has shown limited applicability to nanoparticles because of broad diffraction peak and low diffraction intensity, the μSR is a more sensitive probe for nanoparticles. The bulk CuO is an antiferromagnet with an incommensurate order below $T_{N1}=229$ K, and a commensurate order below $T_{N2}=213$ K.[18–23] When the Cu^{2+} spins in the system is diluted with nonmagnetic ions, the two transition temperatures quickly merge to a single transition temperature of $\sim$200 K.[24–26] Among monoxides, CuO is unique because of its crystallization in a monoclinic structure ($a=4.6837$ Å, $b=3.4226$ Å, $c=5.1288$ Å, $\beta=99.54°$[27]) and its material similarity to superconducting cuprates.[28]

II. SAMPLE PREPARATION AND CHARACTERIZATION

This study investigates antiferromagnetic transitions in two kinds of CuO nanoparticles using μSR and magnetic susceptibility measurements. The μSR measurements require a large quantity of material. For that reason, 10 g of CuO fine particles were prepared by ball milling from pure single crystals of CuO. Single crystals were grown by a chemical vapor transport method, which has been verified to produce high crystal quality and purity.[22,23,28] The present process has eliminated possible contamination caused by magnetic impurities (except for trace amounts of nonmagnetic SiO_2 from the milling balls and vessel). Figure 1(a) shows the synchrotron x-ray diffraction intensity pattern for the ball-milled particles. A conventional method employing the Scherrer relation with instrumental correction produced an average particle size estimation of 8.3 nm.

Electron microscope imaging reveals that these particles are distributed narrowly around 5 nm [Figs. 1(b) and 1(d)]. Detailed investigations using electron diffraction and high-resolution atom imaging showed that they are in crystalline forms other than amorphous. In addition, a surprising result related to ball-milled nanoparticles is that the high-resolution atom imaging revealed no lattice defects that one might expect from the ball-milling process [Fig. 1(d), left panel]. The absence of defects was confirmed by repeated observations. However, a high concentration of defects exists extensively in sub-micrometer particles prepared with the same ball-milling process [Fig. 1(d), right panel]. Although each single observation confirmed only a very small number of particles used for μSR measurements, considering the random sampling for the observation, we presume that the defect-free property is the most probable characteristic of nanoparticles. This conjecture is based on the following arguments. The defects are in a higher energetic metastable state and are pinned by the barrier for moving in bulk crystals. In the nanoparticles, they might readily disappear because of the lack of a pinning mechanism for metastable defects in the nanoparticle lattice.

Another process to grow smaller nanoparticles of CuO is based on a one-step direct synthesis from aqueous solutions of $CuCl_2 \cdot 2H_2O$ and NaOH. By adjusting the concentrations and the ratio of composition of the two compounds, we found that nanoparticles of CuO in rod form (nanorods) were synthesized directly from the solution at room temperature without employing the usual thermal dissociation treatment. The nanorods congregated to appear as large needles at first glance. However, the individual particles were in fact uni-

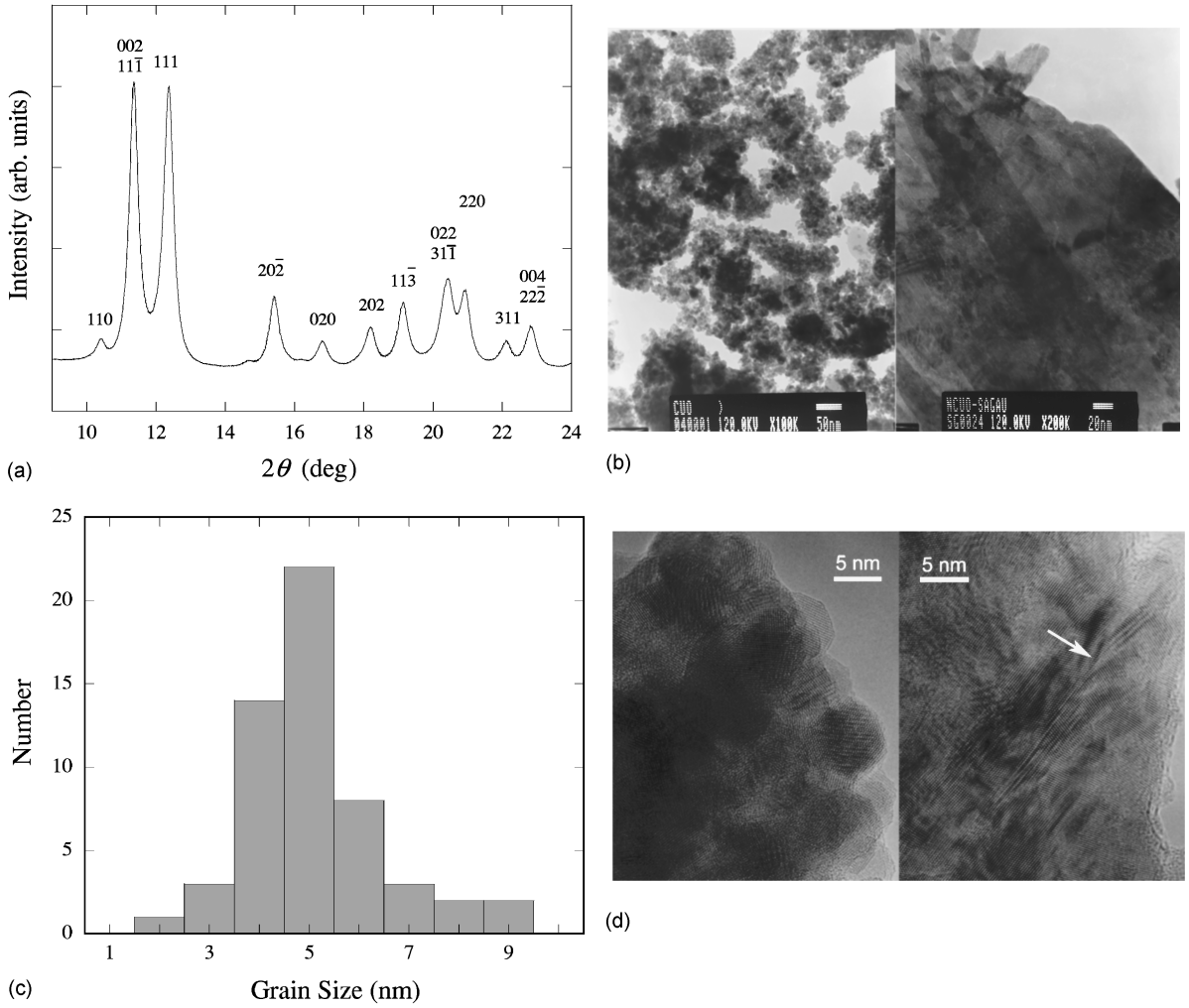

FIG. 1. Synchrotron x-ray ($\lambda = 0.5$ Å) diffraction pattern for ball-milled ~5 nm particles of CuO. (b) Transmission electron microscopy images of ball-milled ~5 nm particles (left) and solution-grown congregated CuO nanocrystals with ~2 to 3 nm diameter (right). (c) Statistical distribution in the nanoparticle size. (d) High-resolution images for the ball-milled nanoparticles (left panel) and ball-milled sub-micrometer particles (right panel). In Fig. (d) defect-free crystalline nanoparticles are apparent at the edges. On the contrary, defects and boundaries exist extensively in the ball-milled sub-micrometer particles, as indicated by the arrow.

formly sized with diameters narrowly distributed around 2 to 3 nm, as shown by electron microscopy in the right panel of Fig. 1(b). Detailed investigation demonstrated that they were good nanocrystals.

Magnetic susceptibility measurements were performed on the two kinds of nanoparticles using a commercial SQUID magnetometer at 1 Tesla. The μSR measurements were carried out on ball-milled nanoparticles at the Meson Science Laboratory, High Energy Accelerator Research Organization (KEK-MSL) using a pulsed surface μ^+ beam with an energy of 20 MeV in a zero field (less than 1 mG) as well as in a longitude external field (LF-μSR). For reference, similar measurements were made of large particles: Sub-micrometer particles that had been similarly prepared by the ball-milling process). The μSR experiment on the nanoparticles was repeated with a continuous surface μ^+ beam at TRIUMF, Canada's National Laboratory for Particle and Nuclear Physics. The asymmetry parameter a of the muon spin at time t, is defined as $a(t)=[F(t)-B(t)]/[F(t)+B(t)]$, where $F(t)$ and $B(t)$ are muon events counted, respectively, by the forward and backward counters. The incident muons are polarized along the longitudinal progressing direction; then the internal fields in the specimen depolarize the initially polarized muons. Thereby, magnetic transitions are directly visible in the muon spectra.

III. RESULTS AND DISCUSSION

In the paramagnetic state, in which relaxation of electron spin is too fast to depolarize the muon spin, the nuclear field (of Cu63 or Cu65 here) dominates depolarization behavior. The asymmetry is known to follow the Kubo-Toyabe function,[29]

$$a(t) = a_0\left[\tfrac{1}{3} + \tfrac{2}{3}(1-\sigma^2 t^2)e^{(-1/2)\sigma^2 t^2}\right] \quad (1)$$

where σ is the distribution width of the nuclear field (1/3 of the muon spins remains the initial longitudinal direction and

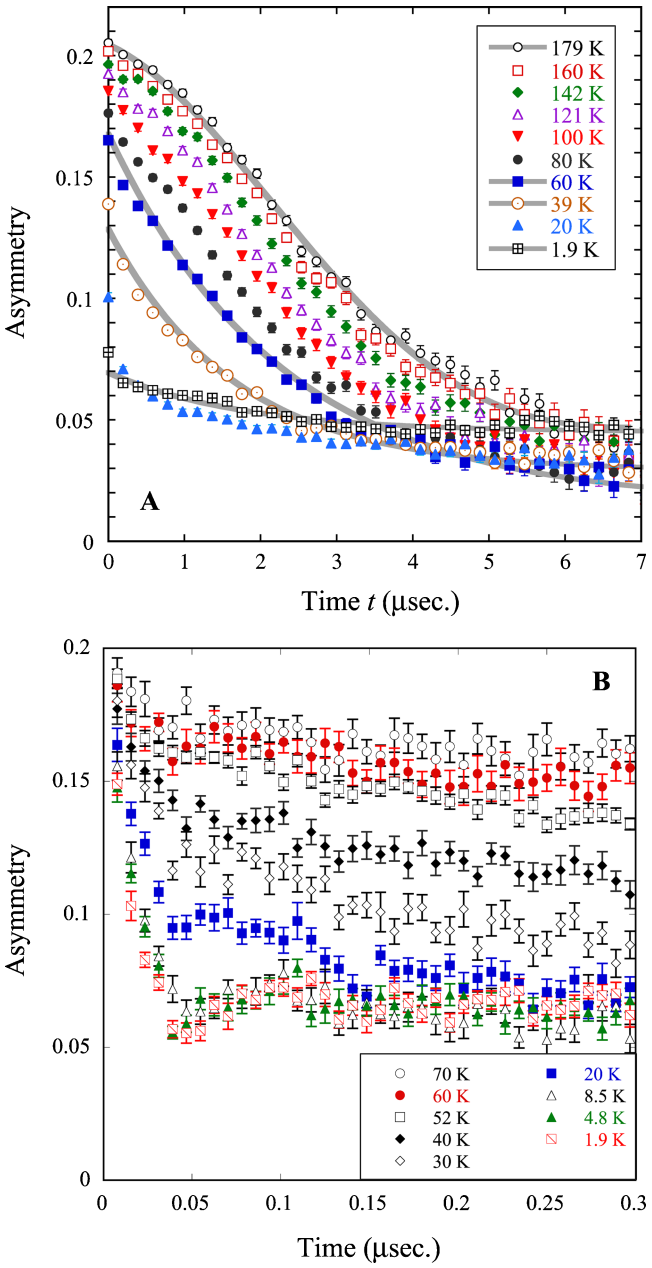

FIG. 2. (Color online) .Time evolution of zero-field μSR asymmetry $a(t)$ for ball-milled ~5 nm particles at typical temperatures with data packing of 500 (a) and 20 (b). Solid lines in (a) are fitted asymmetries.

2/3 muon spins rotate as a result of the influence of the other two vertical components of the field). A static internal field is produced by the ordered spins and the asymmetry decreases rapidly toward a time-independent baseline of 1/3 when a magnetic order is developed inside the specimen. Therefore, the initial asymmetry near $t=0$ might serve as a measure of the magnetic order. The time evolution of the asymmetry $a(t>0)$ reflects the correlation of the spins. Oscillation around the baseline is apparent with the high time resolution of a continuous beam if the magnetic order is long range and the sample is crystallized uniformly.

Figure 2 shows the zero-field μSR spectra with histogram packing of 500 (A) and 20 (B) for the ~5 nm particle assembly at a set of typical temperatures taken at TRIUMF. Few spectra are plotted, thereby allowing a clearer view; hereinafter, except as specifically denoted, the μSR obtained at TRIUMF are presented. In the case of bulk CuO, the initial asymmetry with a histogram packing like that of Fig. 2(a) declined steeply below T_{N2} of 213 K. The muon spin rotation is visible below T_{N2} with packing like that of Fig. 2(b).[30] For the ~5 nm particle assembly, the initial asymmetry began to decrease slightly near 180 K (also refer to Fig. 5), and quickly decreased below around 100 K. Microscopic investigation revealed that the assembly consisted of a dominating majority of fine particles around 5 nm and a few larger particles. Therefore, we attributed the slight decrease above 100 K to the higher T_Ns of the few larger particles. We infer that most particles have T_Ns of less than 100 K. As shown in Fig. 2(b), signs of muon spin rotation indicating the development of a long-range order become evident only below 30 K.

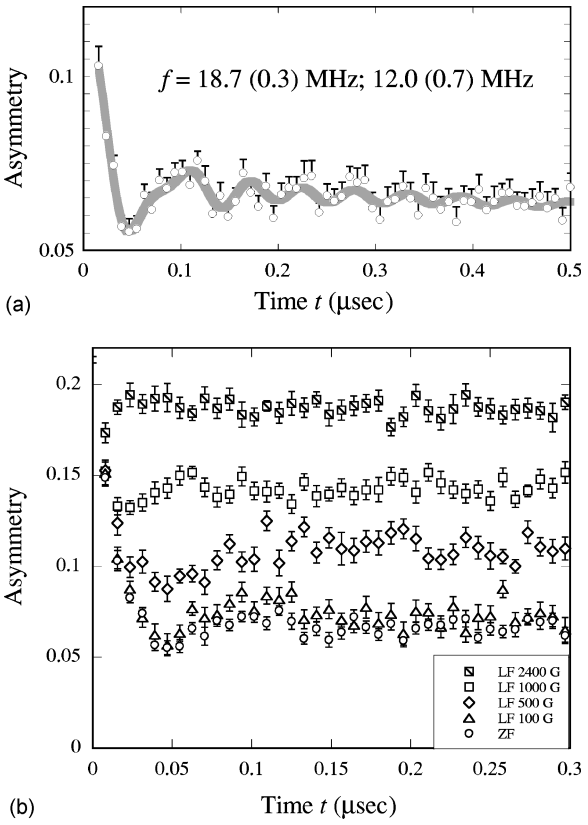

FIG. 3. (a) Oscillation of the muon spin asymmetry for ball-milled ~5 nm particles at 1.9 K showing muon spin rotation. The gray line shows a fit with muon spin rotation frequencies of 18.7 and 12.0 MHz. (b) Time evolution of asymmetries under longitude-fields (LF) at 1.9 K.

Figure 3 shows the time dependence of asymmetry, as measured using ZF-μSR and LF-μSR at 1.9 K and in various fields. The development of long-range order was clearly observed in the ZF-μSR as well as in the LF-μSR. In Fig. 3(a), the ZF-μSR asymmetry is roughly fitted with frequencies of 18.7 (0.3) and 12 (0.7) MHz, which are consistent with the two dominating frequencies of 18.4 and 11.9 MHz in the bulk CuO at low temperatures.[30] The LF-μSR results

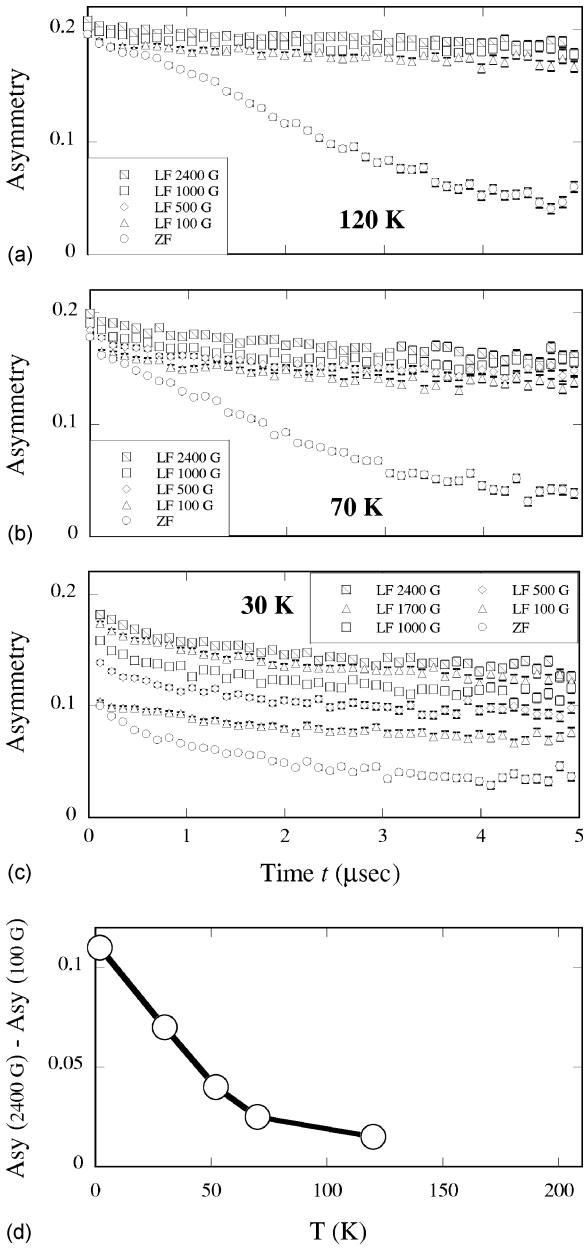

FIG. 4. (a)–(c) Longitude-field (LF) spectra for the ball-milled ~5 nm particles at typical temperatures. (d) Difference asymmetries between 100 G and 2400 G at various temperatures.

shown in Fig. 3(b) unambiguously show the development of a static internal field resulting from a long-range order: The asymmetry recovers in a large external longitude field to cancel the effect of the static internal field.

The LF-μSR a(t) data measured at other temperatures are shown in Fig. 4. At all temperatures, partial decoupling at a weak field of 100 Gauss was observed, suggesting that some nanoparticles remained paramagnetic: In the paramagnetic state, the muon spins are depolarized by the nuclear moments, as shown in Eq. (1), which is decoupled by a weak field of ~100 Oe. Therefore, the difference between decoupling at 2400 and 100 G at the respective temperatures is used as an effective measure of the volume fraction of the antiferromagnetic phase in the nanoparticle assembly. The differences are nearly time-independent. They are plotted versus temperature in Fig. 4(d). That figure shows that the nanoparticle assembly has a distribution of T_N and T_Ns for most of the particles below around 100 K.

Drastic suppression of the antiferromagnetic transition and the distribution of T_N are illustrated more clearly by a quantitative analysis of the ZF-μSR spectra. Their depolarization behaviors, as shown in Fig. 2(a), are well described by a combination of an exponential function with the Kubo-Toyabe function:

$$a(t) = a_0\left[\tfrac{1}{3} + \tfrac{2}{3}(1-\sigma^2t^2)e^{-1/2\sigma^2t^2}\right] * e^{-\lambda t} \qquad (2)$$

Therein, the exponential function expresses depolarization resulting from the magnetic field caused by the electron (Cu^{2+}) spins; a_0 is the initial asymmetry near time zero. The temperature dependence of the fitted a_0, and the depolarization rate λ for the nanoparticle assembly, as well as those for the reference submicrometer particles, are shown in Fig. 5. The sub-micrometer assembly exhibits bulk characteristics. Bulk CuO displays incommensurate order below T_{N1} =229 K and a commensurate order at T_{N2}=213 K, as is proven by the previous reports of neutron studies, magnetic susceptibility studies and μSR studies.[18–23,30] The decrease in a_0 below 230 K for sub-micrometer assembly suggests the start of ordering at T_{N1}. The peak of λ near 210 K is consistent with formation of a long-range order at T_{N2}. In the long-range ordered phase, the $a(t)$ quickly approaches a time-independent constant value (one-third of the initial asymmetry at the paramagnetic state) which reduces λ to zero.

For ~5 nm particles, after a gradual decrease in the initial asymmetry and a gradual increase in the depolarization rate as T decreases, they change at a much faster rate below around 100 K, consistent with the LF-μSR measurements. A plot of the decreasing rate of the initial asymmetry da_0/dT versus the temperature is shown in Fig. 5(c). The rate is highest at 30 K, which indicates that T_N is centered around 30 K. This indication is also consistent with the peak temperature of the depolarization rate λ shown in Figs. 5(a) and 5(b), i.e., implying a T_N of ~30 K for the size of 5 nm.

The Néel temperature of ~30 K of the 5 nm particle assembly is less than one-seventh of the bulk value and exhibits a striking finite-size effect compared with previous reports of direct evidence on CoO or NiO. This result has been further confirmed by our experiments on another nanoparticle assembly with center size of 10 nm (T_N~50 K).[31] It is noteworthy that the drastic reduction is not caused by defects. The ball-milled sub-micrometer particles contain numerous defects, but their T_N has not been changed from the bulk values. On the contrary, these defects were not even observed in the ball-milled nanoparticles with our experiments.

Figure 6 shows magnetic susceptibility measurements (1 Tesla, field cooling) on the ~2 to 3 nm nanorods (20 mg assembly), which display even greater finite-size effect on the smaller nanoparticles. As with previous magnetic susceptibility studies on thin films or nanoparticles with incomplete or amorphous surfaces, our ball-milled nanoparticles showed extrinsic paramagnetic properties because of their surface

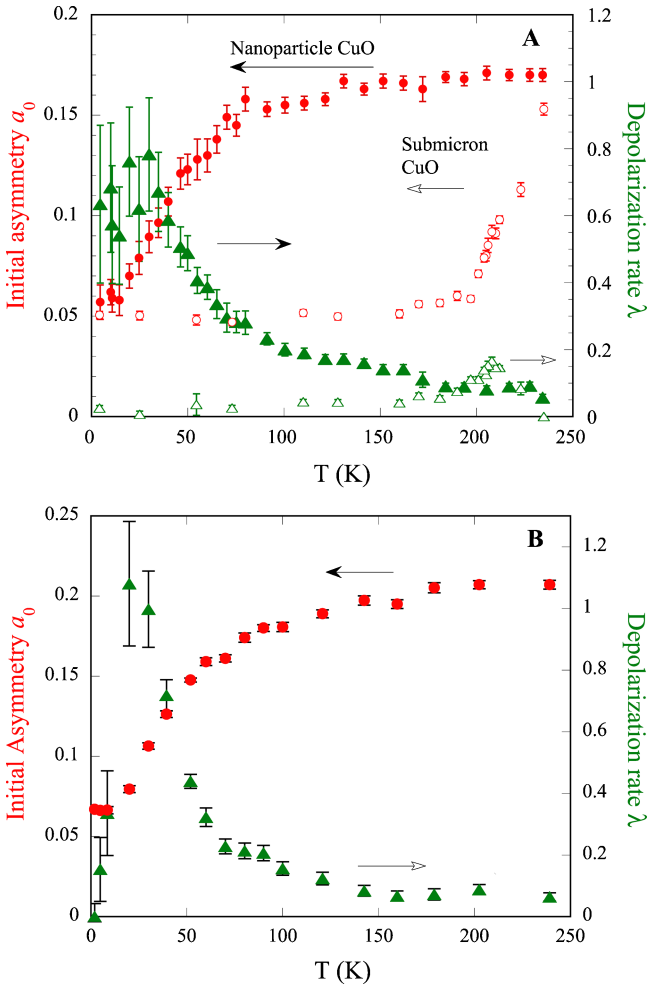

FIG. 5. (Color online) (a) Temperature dependence of the initial asymmetry (filled circles) and depolarization rate λ (filled triangles) for ball-milled ~5 nm particles and the reference ball-milled submicrometer particles (KEK-MSL). (b) Results obtained from a repeated experiment at TRIUMF. (c) The decreasing rate of the initial asymmetries implies a center T_N near 30 K for the ball-milled ~5 nm particles.

states. However, the solution-grown nanocrystals clearly demonstrated an anomaly near 10 K (Fig. 6). For antiferromagnets like CuO, the magnetic transition is better determined from the temperature dependence of $d(\chi T)/dT$.[32,33] As shown in Figs. 7(a) and 7(b), whereas $T_{N1}=229$ K and a $T_{N2}=213$ K are seen for bulk CuO, the T_N of ~13 K for the nanocrystals is observed clearly on the $d(\chi T)/dT-T$ plot. It is noteworthy that no anomaly was observed with the weak field ZFC measurement. These results, combined with those of μSR and susceptibility, and a recent report of T_N of ~170 K for 14 nm CuO,[34] are plotted in Fig. 7(c). This striking reduction in T_N demonstrates the dramatic finite-size effect on the magnetic transition temperature in nanoparticles of CuO when its dimension is reduced to a few nanometers.

A previous study on the magnetic susceptibility measurements of nanoparticle CuO [thermal decomposition of $Cu(OH)_2$ gels] reported an anomaly around 40 K in the magnetic susceptibilities under weak fields for a ~6.6 nm assembly of CuO (determined from the difference between susceptibilities upon field-cooling and ZFC cooling).[33] As shown clearly in the cases of NiO and CoO,[12,13,15] the weak field zero-field-cooling magnetic susceptibility measurements merely reproduce a nonthermodynamic blocking effect. Blocking temperature T_B is influenced by numerous extrinsic parameters such as the grain/layer shape and surface roughness.[17] Low-temperature heating (160 °C in the literature) cannot ensure complete dissociation of $Cu(OH)_2$ and sufficient oxidization to CuO. Consequently, it may produce incomplete surfaces. Actually, we demonstrated in another study that the anomaly in the ZFC magnetic susceptibility is strongly sample-dependent: It may or may not appear.[31]

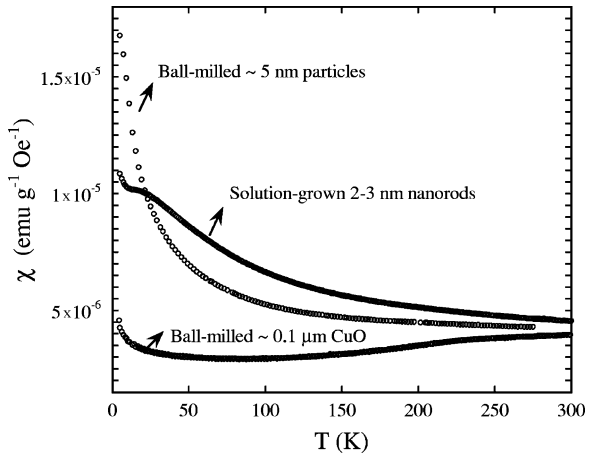

FIG. 6. Temperature dependencies of magnetic susceptibilities for ball-milled ~5 nm particles, solution-grown 2 to 3 nm rods and ball-milled submicrometer particles, respectively.

The zero-field μSR can also detect a superparamagnetic relaxation in magnetic nanoparticles similar as those seen in the zero-field μSR reports on superparamagnetic $Cu_{98}Co_2$.[35] Superparamagnetic relaxation causes the gradual decrease of the initial asymmetry of muon spins in the zero-field μSR spectra and a root-exponential muon depolarization function with an associated relaxation rate that can be related to the mean fluctuation rate of the dipolar fields.[35] Therefore, one might suspect that the decrease in the initial asymmetry of the zero-field μSR in Fig. 2(a) can result from a superparamagnetic relaxation. However, development of muon spin rotations in Figs. 2(b) and 3, the LF-decoupling behavior in Figs. 3 and 4, the peak of the depolarization rate as shown in Fig. 5, and the depolarization of the initial asymmetry to 1/3 the value of that in the paramagnetic state all clearly describe the onset of magnetic order in the nanoparticles. Therefore, the possibility of a superparamagnetic relaxation is excluded in the present CuO nanoparticle study.

The drastic finite size effect might help to solve a relevant problem. Recently, an unusual type of magnetism called superferromagnetism has been reported in one-dimensional and two-dimensional regularly structured arrays of nanostripes of Fe, as well as in self-organized $Co_{80}Fe_{20}$ nanoparticles in multilayers $Co_{80}Fe_{20}/Al_2O_3$.[36,37] For example, nanostripes of iron showed a new "superferromagnetic" transition at 179 K, separate from its Curie temperature above 1000 K. Periodic alignment of the nanoparticles was suggested to produce an unknown inter-particle magnetic coupling. Nevertheless,

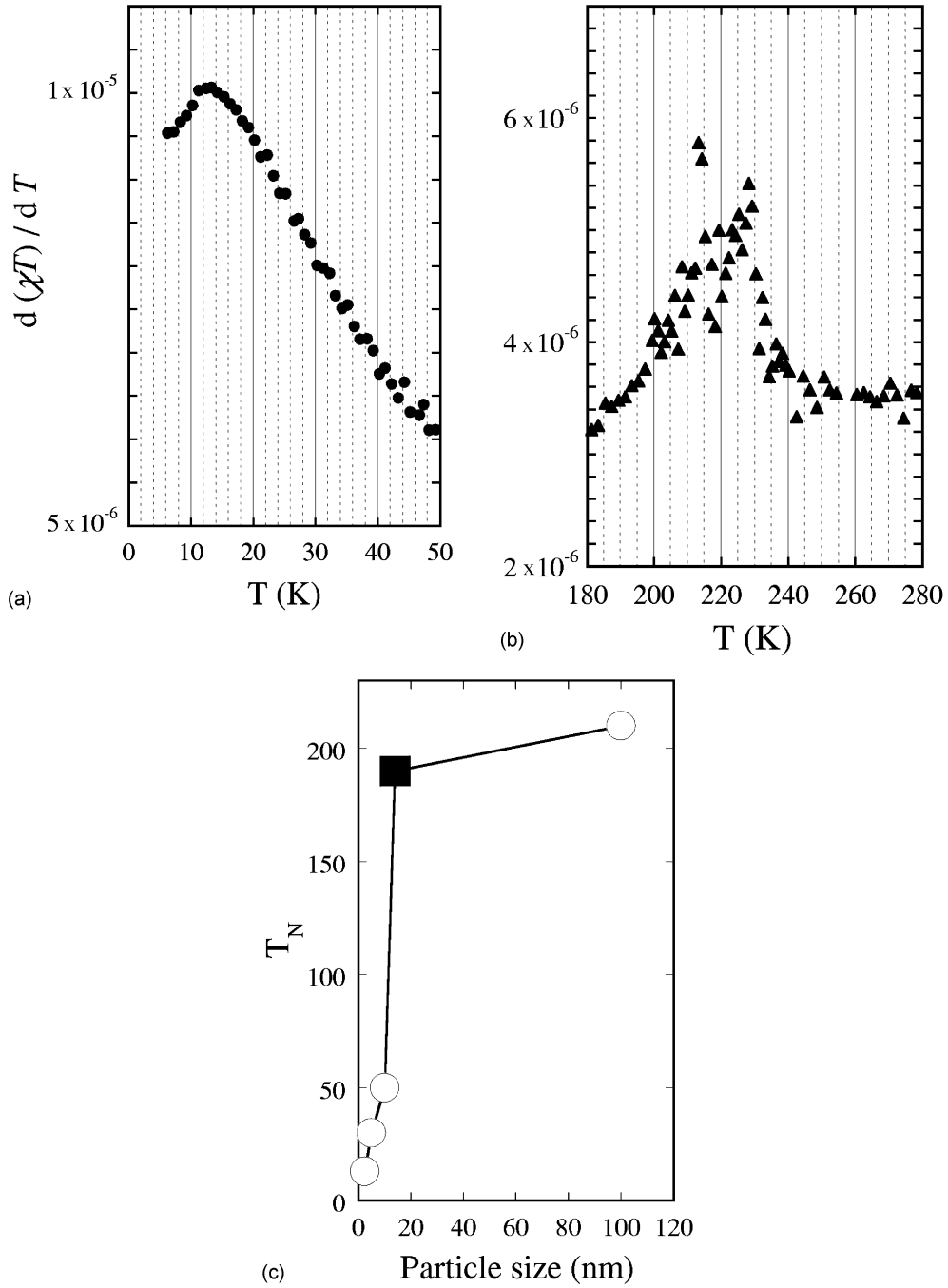

FIG. 7. (a) $d(\chi T)/dT-T$ plot showing $T_N=13$ K for 2 to 3 nm nanocrystal CuO; B: $T_{N1}=229$ K and $T_{N2}=213$ K, respectively, for bulk CuO. (c) Size dependence of the transition temperature T_N for CuO particles (the data for 14 nm CuO (filled square) is taken from Ref. 34).

the same phenomenon appears in randomly decomposed Cu_2MnAl nanoparticles embedded in the $Cu_{64}Mn_9Al_{27}$ alloy.[38] These unusual properties are explainable by assuming a very low T_C because of the finite-size effect.

In summary, the present work reveals a dramatic reduction of the Néel temperature in CuO from the bulk $T_N=229$ K to T_N of ~ 30 K for 5 nm nanoparticles, as well as $T_N=13$ K for 2 to 3 nm nanorods. This dramatic reduction is direct evidence of the drastic finite-size effect on T_N in antiferromagnetic systems. It also lends insight to solving controversial problems of this kind in ferromagnetic systems.

ACKNOWLEDGMENTS

This work was supported by a Grant-in-Aid for Scientific Research to X.G. Zheng from the Japan Society for the Promotion of Science (JSPS Kiban C-15510093). Electron microscopic investigation is supported by the Nanotechnology

Researchers Network Project from the Ministry of Education, Culture, Sports, Science, and Technology, Japan. Synchrotron x-ray experiment was performed at the BL02B2 in the Spring-8 with the approval of the Japan Synchrotron Radiation Research Institute (JASRI) (Proposal No. 2004B0405-ND1d-np). We are grateful to Prof. H. Ogawa, Mr. Y. Mitsuishi at Saga University for providing purified water for sample preparation. The authors thank Dr. Pei-Chun Ho at the University of California, San Diego for reading the manuscript.

*Electronic address: zheng@cc.saga-u.ac.jp

[1] B. Y. Jing and J. B. Ketterson, Adv. Phys. **38**, 189 (1989).
[2] See, e.g., H. Ibach and H. Lueth, *Solid-State Physics*, (Springer, New York, 2000).
[3] C. M. Schneider, P. Bressler, P. Schuster, J. Kirschner, J. J. de Miguel, and R. Miranda, Phys. Rev. Lett. **64**, 1059 (1990).
[4] T. Beier, H. Jahrreiss, D. Pescia, Th. Woike, and W. Gudat, Phys. Rev. Lett. **61**, 1875 (1988).
[5] D. Johnson, P. Perera, and J. O'Shea, J. Appl. Phys. **79**, 5299 (1996).
[6] M. Farle and K. Baberschke, Phys. Rev. Lett. **58**, 511 (1987).
[7] M. Farle, K. Baberschke, U. Stetter, A. Aspelmeier, and F. Gerhardter, Phys. Rev. B **47**, 11571 (1993).
[8] T. Ambrose and C. L. Chien, Phys. Rev. Lett. **76**, 1743 (1996).
[9] Eric E. Fullerton, K. T. Riggs, C. H. Sowers, S. D. Bader, and A. Berger, Phys. Rev. Lett. **75**, 330 (1995).
[10] Sanshiro Sako and Kazunari Ohshima, J. Phys. Soc. Jpn. **64**, 944 (1995).
[11] Sanshiro Sako, Kazunari Ohshima, Masahiro Sakai, and Shunji Bandow, Surf. Rev. Lett. **3**, 109 (1996).
[12] E. N. Abarra, K. Takano, F. Hellman, and A. E. Berkowitz, Phys. Rev. Lett. **77**, 3451 (1996).
[13] Y. J. Tang, David J. Smith, B. L. Zink, F. Hellman, and A. E. Berkowitz, Phys. Rev. B **67**, 054408 (2003).
[14] S. N. Klausen, P.-A. Lindgard, K. Lefmann, F. Bødker, and S. Møorup, Phys. Status Solidi A **189**, 1039 (2002).
[15] P. J. van der Zaag, Y. Ijiri, J. A. Borchers, L. F. Feiner, R. M. Wolf, J. M. Gaines, R. W. Erwin, and M. A. Verheijen, Phys. Rev. Lett. **84**, 6102 (2000).
[16] L. Néel, in *Low Temp. Phys.*, edited by C. Dewitt, B. Dreyfus, and P. G. de Gennes (Gordon and Beach, New York, 1962), p. 413.
[17] Review papers: J. Nogues and Ivan K. Schuller, J. Magn. Magn. Mater. **192**, 203 (1990); A. E. Berkowits and Kentaro Takano, *ibid.* **200**, 552 (1990).
[18] J. B. Forsyth, P. J. Brown and B. M. Wanklyn, J. Phys. C **21**, 2917 (1988).
[19] B. X. Yang, T. R. Thurston, J. M. Tranquada, and G. Shirane, Phys. Rev. B **39**, 4343 (1989).
[20] P. J. Brown, T. Chattopadhyay, J. B. Forsyth, V. Nunez, and F. Tasset, J. Phys.: Condens. Matter **3**, 4281 (1991).
[21] M. Ain, A. Menelle, B. M. Wanklyn, and E. F. Bertaut, J. Phys.: Condens. Matter **4**, 5327 (1992).
[22] X. G. Zheng, C. N. Xu, Y. Tomokiyo, E. Tanaka, H. Yamada, Y. Soejima, and Y. Yamamura, and T. Tsuji, J. Phys. Soc. Jpn. **70**, 1054 (2001).
[23] X. G. Zheng *et al.*, J. Appl. Phys. **92**, 2703 (2002).
[24] X. G. Zheng, H. Yamada, Daniel J. Scanderbeg, M. B. Maple, and C. N. Xu, Phys. Rev. B **67**, 214516 (2003).
[25] K. Saito, S. Ikeuchi, Y. Nakazawa, X. G. Zheng, M. B. Maple, and M. Sorai, Solid State Commun. **125**, 23 (2003).
[26] X. G. Zheng, Y. Kodama, Kazuya Saito, E. Tanaka, Y. Tomokiyo, H. Yamada, and C. N. Xu, Phys. Rev. B **69**, 094510 (2004).
[27] S. Asbrink and L. J. Norrby, Acta Crystallogr., Sect. B: Struct. Crystallogr. Cryst. Chem. **26**, 8 (1970).
[28] X. G. Zheng, C. N. Xu, Y. Tomokiyo, E. Tanaka, H. Yamada, and Y. Soejima, Phys. Rev. Lett. **85**, 5170 (2000).
[29] R. Kubo and T. Toyabe, *Magnetic Resonance and Relaxation*, edited by R. Blinc (North-Holland, Amsterdam, 1967), p. 810.
[30] K. Nishiyama, W. Higemoto, K. Shimomura, A. Koda, G. Maruta, S. W. Nishiyama, and X. G. Zheng, Hyperfine Interact. **136/137**, 289 (2001).
[31] X. G. Zheng, T. Mori, K. Nishiyama, W. Higemoto, and C. N. Xu, Solid State Commun. **132**, 493 (2004).
[32] E. E. Bragg and M. S. Seehra, Phys. Rev. B **7**, 4197 (1973).
[33] A. Punnoose, H. Magnone, M. S. Seehra, and J. Bonevich, Phys. Rev. B **64**, 174420 (2001).
[34] S. J. Stewart, M. Multigner, J. F. Marco, F. J. Berry, A. Hernando, and J. M. Gonzalez, Solid State Commun. **130**, 247 (2004).
[35] R. I. Bewley and R. Cywinski, J. Magn. Magn. Mater. **177-181**, 923 (1998); Phys. Rev. B **58**, 11544 (1998).
[36] M. R. Scheinfein, K. E. Schmidt, K. R. Heim, and G. G. Hembree, Phys. Rev. Lett. **76**, 1541 (1996).
[37] X. Chen, O. Sichelschmidt, W. Kleemann, O. Petracic, C. Binek, J. B. Sousa, S. Cardoso, and P. P. Freitas, Phys. Rev. Lett. **89**, 137203 (2002).
[38] G. A. Takzei, I. Mirebeau, L. P. Gun'ko, I. I. Sych, O. B. Surzhenko, S. V. Cherepov, and Yu. N. Troschenkov, J. Magn. Magn. Mater. **202**, 376 (1999).